Electrochemical Detection of Dopamine and Riboflavine on a Screen-Printed Carbon Electrode Modified by AuNPs Derived from *Rhanterium suaveolens* Plant Extract

Sabrine Chelly, Meryam Chelly, Rayhane Zribi, Radhouane Gdoura, Hanen Bouaziz-Ketata, and Giovanni Neri*

ACCESS | Metrics & More | Article Recommendations

ABSTRACT: A AuNP-modified screen-printed carbon electrode (AuNP/SPCE) for monitoring important biomolecules, such as dopamine (DA) and riboflavin (RF), having a high potential for personalized medicine and for continuous monitoring of human health is here proposed. AuNPs were synthesized using the extract of *Rhanterium suaveolens* as a reducing medium and were characterized by UV−vis spectroscopy, dynamic light scattering (DLS), and scanning and transmission electron microscopy (SEM and TEM). The synthesized AuNPs appear spherical and present a bimodal size distribution with a maximum centered at around 30−50 nm. Cyclic voltammetry (CV) experiments demonstrated that the modified AuNP/SPCE sensor exhibits superior electrochemical performances to the bare SPCE. Low limits of detection (LODs) of 0.2 and 0.07 μM at S/N = 3 and sensitivities of 550.4 and 2399 μA mM^{-1} cm^{-2} were registered for DA and RF detection, respectively. Results demonstrate the promising electrochemical characteristics of the synthesized AuNPs and developed AuNP/SPCE electrochemical sensor for the determination of these important biomolecules.

1. INTRODUCTION

In recent years, researchers are frequently looking at the use of natural ecological sources for producing nanomaterials for a variety of applications.[1] For example, natural bioresources have attracted significant attention for the preparation of electrode materials, conductive supports, and additives for electrodes, which are of high interest in the realm of electrochemical applications.[2] To be specific, the synthesis of metal nanoparticles with outstanding electrocatalytic properties is of prominent interest for the development of novel electrochemical sensors.[3] The conventional methods for metal nanoparticle synthesis are generally expensive and often involve the use of complex procedures, which may pose many limitations for practical applications. Therefore, researchers have devoted recently their attention to the development of more efficient and simple methods for their synthesis.[4] The production of metal nanoparticles using plant extract as a reducing agent is considered a viable alternative to conventional chemical and physical methods.[5] In addition, the method allows the large-scale production of metal nanoparticles at a faster rate and in various shapes and sizes in comparison with metal nanoparticles produced by other methods.[6] Despite these advantages, more work is needed to make reliable the preparation of nanoparticles by means of this method. In particular, there are still many factors to be better understood; for example, the knowledge of the main reducing substances present in the extract should be known so that a precise and repeatable method can be established.

Gold nanoparticles (AuNPs) have received much attention in the last years in the electrochemical field because of their interesting properties, such as large surface-to-volume ratio, high biocompatibility, high stability, and fast electron transfer.[7] To fit the scope, AuNPs have been synthesized by different chemical and physical methods.[8,9] Owing to their importance, many efforts have been dedicated to the synthesis of AuNPs by utilizing various plant extracts.[10] For example, plant extract from *Aloe vera* has been utilized in the synthesis of AuNPs owing to its high content of reducing agents.[11] Green synthesis of AuNPs was reported using *Centella asiatica* extract,[12] *Magnolia kobus* and *Diopyros kaki*,[13] pear fruit extract,[14] and *Rhodo pseudomonas*[15] and *Cape aloe* active components.[16] The efficacy of these plant extracts has been related to the presence of a large variety of substances with high reducing activity, such as polyphenols. These latter are considered good reducing
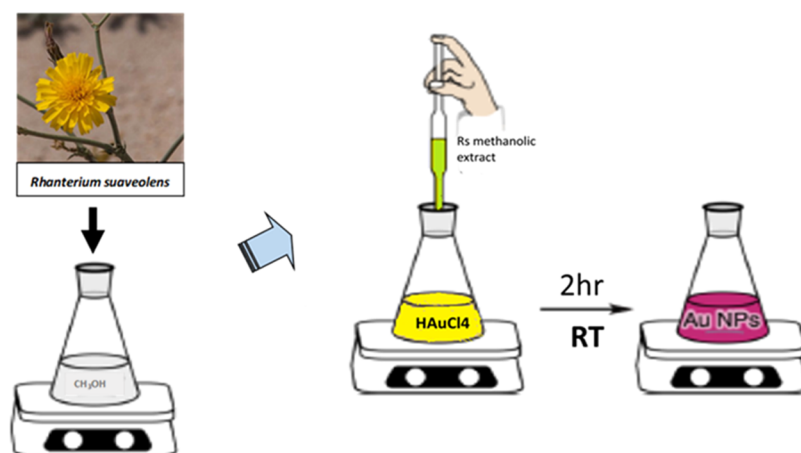
Scheme 1. Schematic Procedure for the Preparation of AuNPs

agents for synthesizing metal nanoparticles due to the presence of carboxyl groups and hydroxyl groups in their molecules.[17]

In the present study, the green synthesis of AuNPs has been carried out using the plant extract of *Rhanterium suaveolens*. Among the other phytochemicals present in the extract of this plant, a number of phenolic compounds have been also identified. The profile of these phenolic compounds has been reported in a previous paper.[18] Some of these, such as p-coumaric acid and ferulic acid, are present in high amounts and can act as reducing and stabilizing agents during the synthesis of AuNPs.[19]

AuNPs play a key role in the recent advances in biomedical applications.[20] Along with biocompatibility, the electrochemical properties of gold nanoparticles have attracted significant attention for a wide range of biosensing applications. Among these, the development of electrochemical sensors for the quantification of biomolecules in physiological fluids, such as dopamine (DA) and riboflavin (RF), is an important scientific and applicative research field with implications in human health. Dopamine (DA) is a neurotransmitter playing a crucial role in our body, regulating cognitive processes such as attention and working memory by acting on a range of receptors in the brain. Alterations in the DA concentration have a strong association with different neurodegenerative diseases such as Parkinson's.[21] Riboflavin (RF), also called vitamin B2, is the major component of the cofactors flavin adenine dinucleotide (FAD) and flavin mononucleotide (FMN), and it is required for a variety of enzyme reactions including activation of other vitamins. Vitamin B2 is an essential component of the human diet; it plays indeed a key role in energy production from carbohydrates, acids, and fats for the body and can be found in many foods such as milk, meat, eggs, nuts, enriched flour, and green vegetables.[22]

Due to their importance, a large variety of analytical techniques have been proposed for monitoring these biochemical substances. On the other hand, conventional analytical methods are generally time-consuming and need complicated sample processing and procedures, high-cost instruments, and well-trained personnel. Electrochemical sensors are instead much more simple, cheaper, easy to use, and suitable to be implemented in lab-on-chip devices. Many electrochemical sensors have been then developed in recent years for dopamine and riboflavin sensing with the sensitivity, selectivity, and accuracy suitable for their use in food and

biomedical applications.[23−33] However, only a few electrochemical sensors have been reported so far for simultaneous determination of dopamine and riboflavin. Furthermore, they rely on complicated electrode modifications by composites to improve the electrochemical response or deposition on glassy carbon electrodes.

The use of screen-printed carbon electrodes (SPCEs), which are inexpensive, smaller, and suitable for mass production by thick-film technology, make simpler the fabrication of electrochemical sensors for testing their possible practical applications.[34,35] Therefore, here, we proposed a novel screen-printed platform modified by gold nanoparticles. Its enhanced performances have been investigated in the electrochemical analysis of dopamine and riboflavin and correlated to the large effective surface area, fast mass transport, and effective electrocatalysis of AuNPs synthesized by the simple method proposed. The presently developed sensor was able to determine riboflavin in real samples such as pharmaceutical formulations.

2. RESULTS AND DISCUSSION

2.1. AuNP Preparation and Characterization. The procedure for the synthesis of AuNPs is illustrated in Scheme 1. First, the methanolic extract of *R. suaveolens* was obtained as described in detail in Section 3 and in a previous paper.[18] Then, it was added, drop by drop and under stirring conditions, to the solution of $AuCl_4^-$ ions. Initially, the $HAuCl_4$ solution had a pale yellow color and a pH of 4.5. Within 15 min, the color changed to purple-red, indicating the fast reduction of Au ions.

The course of the reaction was monitored by UV−vis in the 425−675 nm range, following the increase of the characteristic plasmonic resonance band (see Figure 1a) due to the formation of gold nanoparticles.[36] A rapid increase in the intensity of the plasmon absorption band was initially observed. This is in accordance with the fact that in an acidic medium the reduction of gold ions occurs at a very fast rate.[37] As the reaction proceeded, the concentrations of $AuCl_4^-$ ions decreased, leading to an increase of the solution pH. Preliminary experiments carried at an almost neutral pH value (i.e., 7.4) evidenced that the equilibrium between the gold ions present in the solution is shifted toward gold hydroxo complexes, which are in fact reduced at a lower rate. By following the intensity of the plasmon absorption band centered at 530 nm, the reduction reaction appears to be
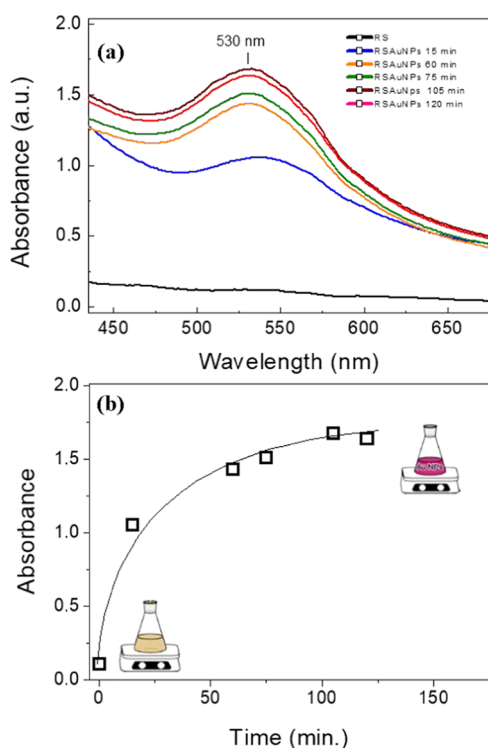
Figure 1. (a) UV–vis spectrum of the reaction mixture at different reaction times. (b) Trend of the intensity of absorbance measured at the maximum of the Au plasmonic resonance vs the reaction time.

completed after about 100 min (see Figure 1b). From the well-known relationships between the plasmon resonance peak and gold particle size,[36] an average size of 47 nm was calculated.

This value was compared with those obtained independently from other techniques, i.e., dynamic light scattering (DLS), scanning electron microscopy (SEM), and transmission electron microscopy (TEM). DLS measurements (Figure 2) show a bimodal distribution with the majority of AuNPs having a particle size in the range between 20 and 50 nm. The second component of larger particle size, in the range 100–300 nm, is also identified in the DLS pattern, even if takes into account only a minority of AuNPs. These findings are also confirmed by SEM analysis (see the inset in Figure 2), showing round Au particles of around 30–50 nm diameter. However, some larger particles, extending up to 100 nm, are also
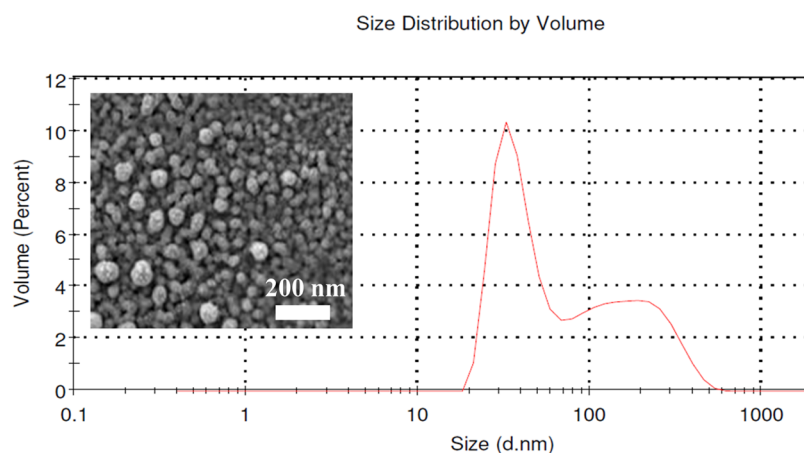
observed. The much larger size of the AuNPs measured using DLS, as compared to SEM analysis, is due to the well-known overestimation of particle size by the DLS technique, which provides information about the hydrodynamic diameter rather than the actual diameter of AuNPs.[38]

The AuNP sizes here obtained fell within the range of values reported in the literature. Most of the studies on the biosynthesis of AuNPs from plant extracts report sizes of the obtained AuNPs between 10 and 50 nm, depending on different process parameters like the effect of pH, stirring conditions, temperature, and concentrations of plant extract and gold ions.[39]

The characterization of AuNPs has been extended also on the nanoparticles deposited on the working carbon electrode to fabricate the modified AuNP/SPCE. The surface morphology of the carbon working electrode of bare SPCE is shown in the SEM micrograph reported in Figure 3a.

The porous structure of the working electrode is clearly visible (see also the inset in Figure 3a, which shows high magnification of the working electrode surface), and this may help to maintain the AuNPs in a highly dispersed state. TEM-EDX analysis reported in Figure 3b,c shows the nanoparticles on the surface of the carbon electrode. EDX mapping (red color in Figure 3c is the signal coming from the Au element) confirms that nanoparticles seen in TEM images of Figure 3b are AuNPs covering the surface of the working carbon electrode. They appear to have a spherical shape and a large particle size variability as deduced before by SEM and DLS measurement.

2.2. Electrochemical Tests. The electrochemical behavior of the bare SPCE and modified AuNP/SPCE (or RSAuNP/SPCE, where it is specified that AuNPs have been synthesized using the *R. suaveolens* (RS) extract) was evaluated by cyclic voltammetry (CV) in 1 M phosphate buffer solution (PBS) at a scan rate of 50 mV s^{-1}. Figure 4 shows the cyclic voltammograms of both electrodes in 10 mM $K_3Fe(CN)_6$. On bare SPCE, a reversible voltammogram for the redox couple $Fe(CN)_6^{3-}/Fe(CN)_6^{4-}$, showing a pair of well-defined redox peaks with the anodic and cathodic peak potentials of 0.400 and −0.176 V, respectively, and a peak potential difference of 576 mV, was observed.

Cyclic voltammograms of the modified AuNP/SPCE electrode appear to be increased in intensity; furthermore, the peak difference is somewhat reduced (354 mV). This
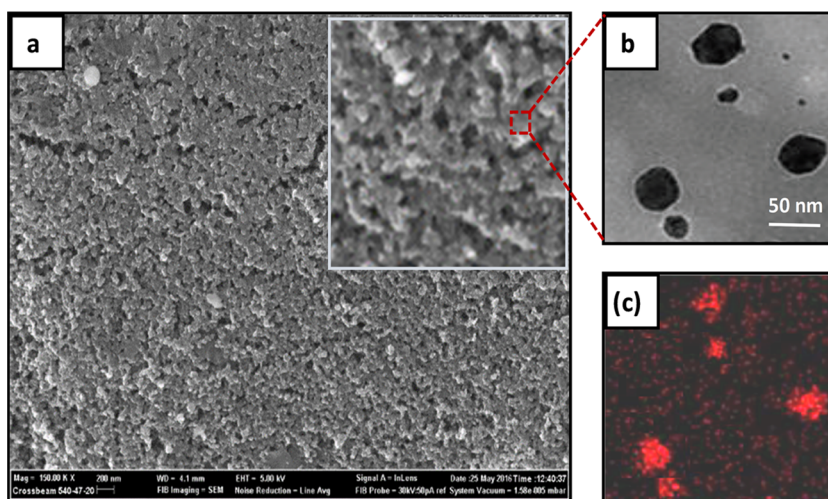

Figure 2. DLS spectrum of AuNPs in diluted aqueous solution. The inset shows the SEM image of AuNPs in the powder form.

Figure 3. (a) SEM image showing the surface of SPCE. The inset in (a) shows high magnification of the surface of the carbon electrode. (b) TEM image showing AuNPs on the surface of the carbon electrode. (c) Energy-dispersive X-ray (EDX) mapping image.
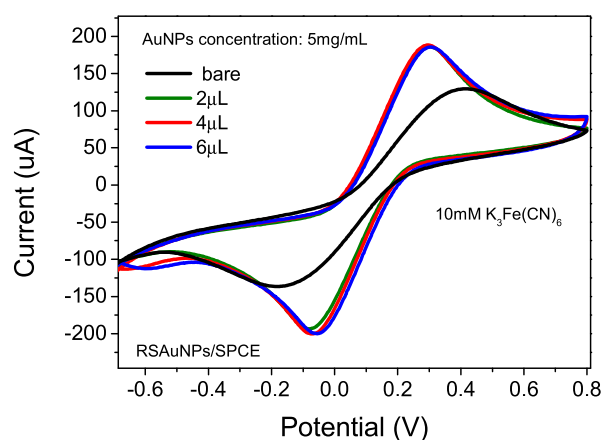

Figure 4. Cyclic voltammograms of bare SPCE and modified SPCE with different loading amounts of dipped AuNPs. The scan rate is 50.0 mV s^{-1} in 10.0 mM K$_3$Fe(CN)$_6$ containing 100.0 mM KCl.

indicates that AuNPs help electron transfer reaction and also favor the redox reaction.

Because the number of AuNP layers deposited on the working electrode influences the electrochemical detection, to optimize this parameter, we prepared a dispersion of AuNPs at a concentration of 5 mg mL^{-1}; then, we loaded the working electrode with different amounts of AuNPs by using different volumes (2, 4, and 6 μL) of the prepared dispersion. The electrode loaded with 2 μL of AuNP dispersion dipped on SPCE has demonstrated an optimal response considering its lower nanoparticle loading with respect to the other electrodes.

Then, electrochemical tests were carried out in the presence of dopamine and riboflavin. Figure 5a presents the cyclic voltammograms obtained for the bare SPCE and modified AuNPsSPCE, respectively in the absence and presence of dopamine. Whereas no peak has been observed on these electrodes in the absence of dopamine, SPCE shows an oxidation peak at around 105 mV vs Ag/AgCl in the presence of dopamine. It is clearly noted that, on modified AuNP/SPCE, the oxidation peak has been shifted to negative potential compared to that on the bare electrode. The oxidation peak is at around 80 mV vs Ag/AgCl, and also, it presents a significantly higher intensity than that on bare
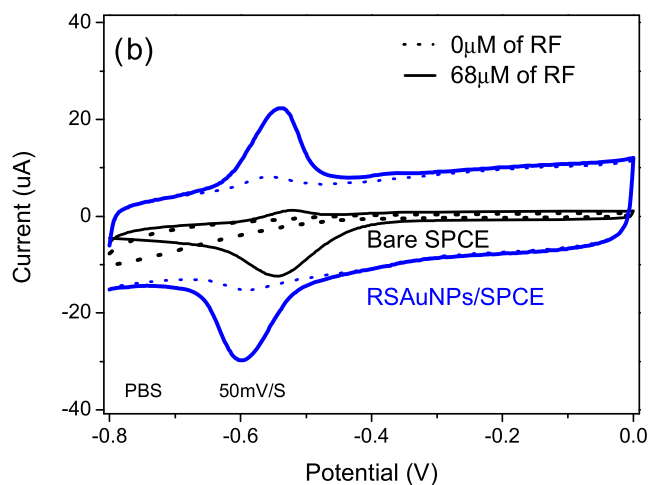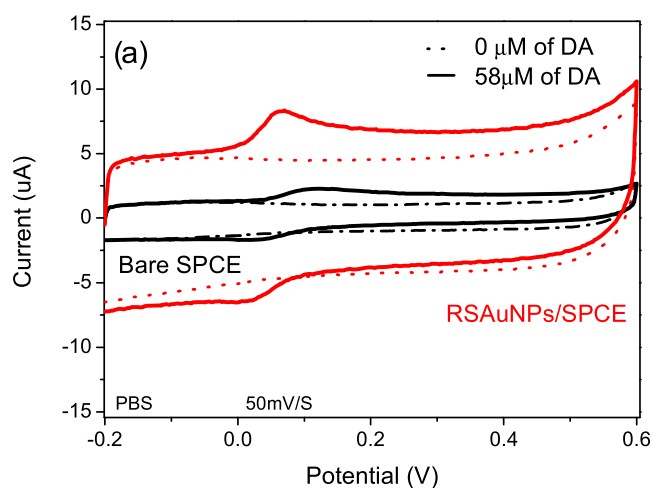
Figure 5. Electrochemical behavior of the AuNP-modified electrode in the absence and presence of (a) DA and (b) RF. CV was performed in 1 M PBS electrolyte at a scan rate of 50 mV s^{-1}.

SPCE. These findings reveal that AuNP/SPCE has a better electrocatalytic effect on dopamine.

Figure 5b presents the cyclic voltammograms obtained for the bare SPCE and modified AuNP/SPCE in the absence and presence of riboflavin. CV curves obtained in the presence of
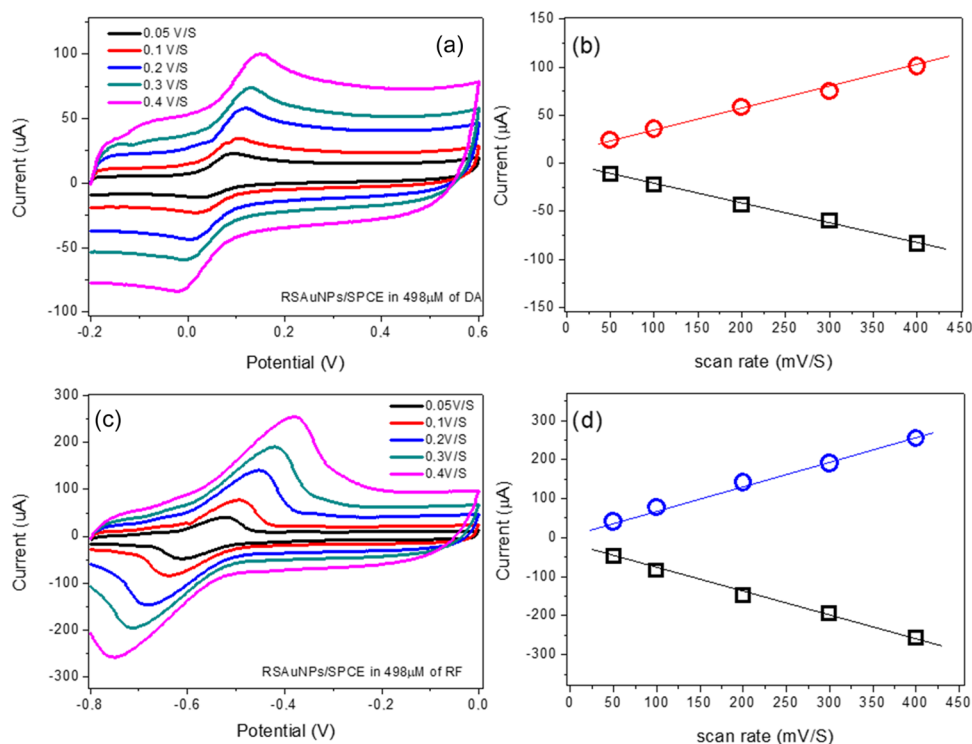
Figure 6. Effect of scan rate from 0.05 to 0.4 V s^{-1} on cyclic voltammograms of AuNP/SPCE of (a, b) 500 μM DA and (c, d) 500 μM RF.
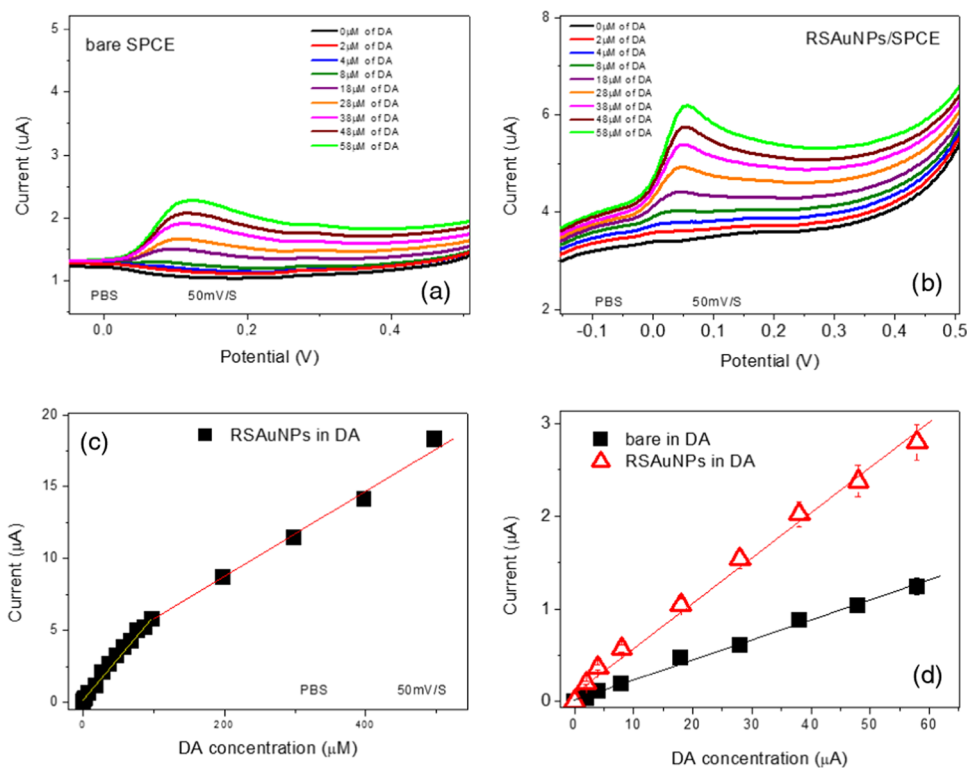

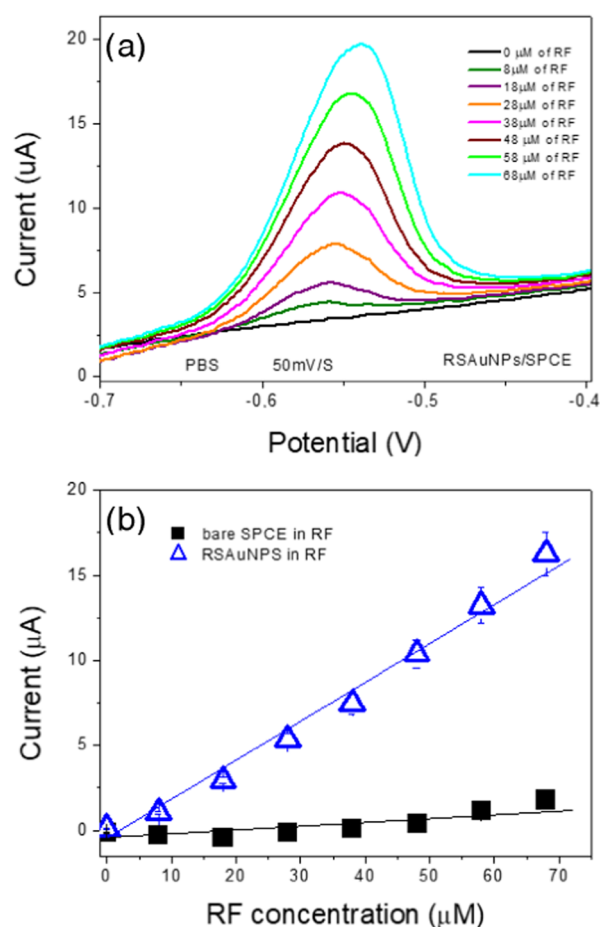**Figure 7.** (a) LSV curves for bare SPCE, performed in 0.1 M PBS electrolyte and in the presence of different concentrations of DA (0−60 μM). (b) LSV curves for AuNP/SPCE, performed in 0.1 M PBS electrolyte and in the presence of different concentrations of DA (0−60 μM). (c) Calibration curve for the determination of DA in the range 0−500 μM. (d) Calibration curve for the determination of DA in the range 0−60 μM.

riboflavin are characterized by the presence of a pair of peaks at −0.52 and −0.54 V on the bare SPCE and at −0.5361 and −0.601 V on the AuNP-modified electrode, which are related to the reversible oxidation/reduction process of RF on the electrode surface. However, on the SPCE electrode, the anodic

peak intensity is very low, suggesting low electrocatalytic activity of the unmodified electrode for the oxidation reaction of RF. The behavior of the modified AuNP/SPCE is similar to that previously described for dopamine. The best performances of the modified electrode can be associated with an increase of

the effective surface area of the working electrode, which leads to an improvement of the electrocatalytic oxidation activity toward these analytes. This is confirmed by the fact that, compared to bare SPCE, AuNP/SPCE exhibits a larger CV cycle, which can be associated with the higher surface area of the AuNP-modified electrode.

Studies were also performed while monitoring the current peak as a function of the scan rate (ν) in the range of 50−400 mV s^{-1} (Figure 6a,c) in 1 M PBS containing DA and RF.

For both analytes, the anodic and cathodic peak currents increased linearly with the scan rate (Figure 6b,d), indicating the occurrence of a redox process involving surface-confined species.[40] As can be seen, by increasing the scan rate, the anodic and cathodic peak potentials shifted toward positive and negative directions, indicating charge-transfer kinetics limitations.

2.3. Electroanalytical Characteristics of the AuNP/SPCE Electrode.

Owing to the good electrochemical characteristics of the AuNP/SPCE, we investigate its electroanalytical properties toward the quantitative determination of DA and RF by the linear sweep voltammetry (LSV) technique (Figures 7 and 8).

Looking at the LSV curves for the bare and modified electrode (Figure 7a,b, respectively), it can be noted the strong increase of dopamine anodic peak current when the SPCE electrode is modified with AuNPs. A linear increase of the current peak intensity was recorded by increasing the DA concentration in the range from 0 to 60 μM (Figure 7c). This has been verified also by tests performed in a larger interval of DA concentration (from 0 to 500 μM). The calibration curve for dopamine on the AuNP/SPCE (Figure 7c) shows two distinct linear regions: one at a lower concentration (from 0 to 100 μM) and another at a higher concentration (100−500 μM). Figure 7d highlights the almost threefold increase of sensitivity in the first linear region obtained with the modified sensor compared to that with bare SPCE. The calibration curve from the above measurements carried in the linear range of lower concentrations shows a sensitivity (as extracted from the slope of calibration plot) of 550.4 μA mM^{-1} cm^{-2} and a determination coefficient (R^2) of 0.9934. The limit of detection was determined as 0.22 μM considering a signal-to-noise ratio (S/N) of 3.

A strong enhancement of the sensor performances has been evidenced for the monitoring of riboflavin, too (see Figure 8a,b). LSV curves registered with the modified sensor are in fact well defined also at the lower RF concentrations and resulted in an almost tenfold increase of the riboflavin anodic peak current with respect to bare SPCE.

By the linear relationship (R^2 = 0.938) between current intensity and riboflavin concentration in the range from 0 to 70 μM, the calculated sensitivity resulted to be 2399.3 μA mM^{-1} cm^{-2}. The limit of detection (LOD) estimated from the calibration curve for the sensor was 0.067 μM (at S/N = 3).

Subsequently, the simultaneous electrochemical detection of DA and RF was also examined by linear sweep voltammetry (LSV). Figure 9a shows the LSV curve, where two clear anodic peaks, attributed to the oxidation of DA and RF, can be easily identified and simultaneously detect using LSV. Quantitative data (not shown) demonstrated further that the anodic peak current of DA increased linearly by the addition of DA in the presence of UA kept constant. On the other hand, the oxidative peak current of UA increased linearly by the addition of a known amount UA in the presence of DA kept constant.

In addition, Figure 9b shows the LSV pattern of a DA and RF mixture solution in the presence of AA and UA. Ascorbic acid and riboflavin occur together in many pharmaceutical preparations and food products. The anodic current peak of individual DA and RF resulted in almost no change in the presence of these other electroactive species, suggesting the anti-interference capability of the modified electrode in the case of concurrent determination of DA and RF in a complex sample containing AA and UA, such as biological fluids in pharmaceuticals and many foods. In addition, in practical applications, these and many other substances present in real samples can cause interferences with the determination of the target analyte. Interferent substances depend, of course, on the real sample considered. For example, both DA and RF are used largely in pharmaceutical formulations, so they can be found as pollutants in wastewater. In this application, main interferences are possible due to the ions present in wastewater, such as Ca^{2+}, Mg^{2+}, K$^+$, Cl$^-$, and Na$^+$, along with a variety of other pollutant organic molecules (sugars, phenols, other vitamins, etc.). As demonstrated in a previous paper using modified electrodes with AuNPs coming from another plant extract, the amperometric signal of the DA and RF analytes is not influenced by the presence of the above substances.[41] Further, the same indication can be inferred from the CV technique analysis reported above in Figure 9b.

Figure 8. (a) LSV curves for AuNP/SPCE, performed in 0.1 M PBS electrolyte and in the presence of different concentrations of RF (0−70 μM). (b) Calibration curves obtained with the bare SPCE and AuNP/SPCE for the determination of RF in the range 0−70 μM.
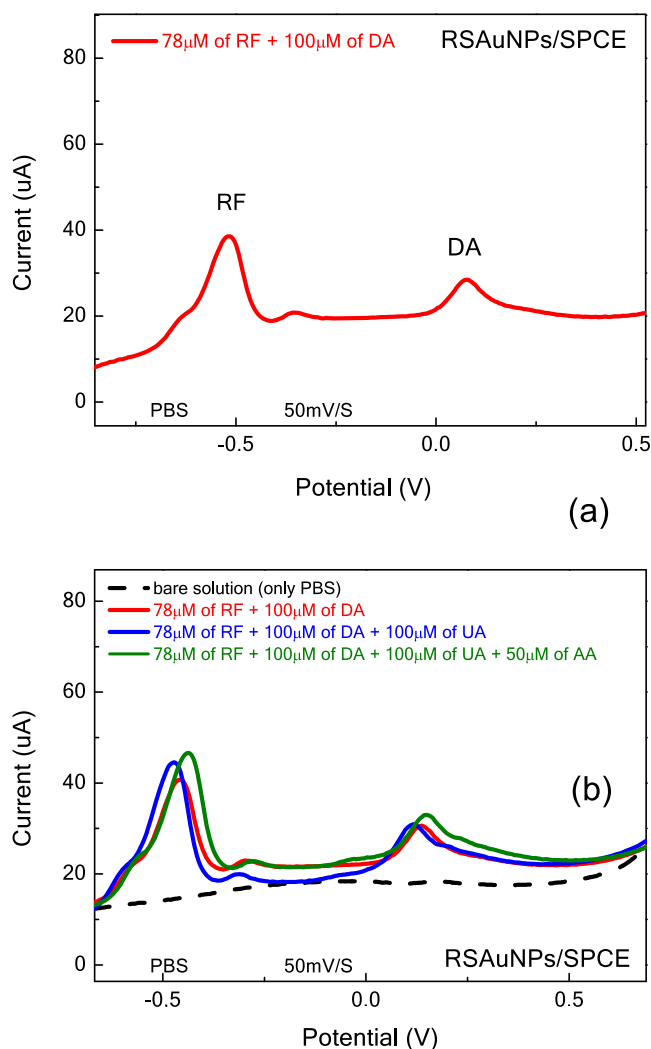
(a)

(b)

Figure 9. (a) LSV curve showing the well-separated anodic peaks attributed to the oxidation of DA and RF. (b) LSV curves of the DA and RF mixture solution in the presence of AA and UA.

The stability of the developed modified sensor has been also tested. This assumes high importance because electrode fouling is commonly encountered with conventional solid electrodes used for the oxidation of DA. The repeatability of the fabricated AuNP/SPCE sensors was investigated by performing a series of repetitive measurements using the same electrode in the presence of DA or RF. The applied statistical analysis, carried out by evaluating the relative standard deviation (RSD), has shown that the response repeatability of the AuNP electrode is pretty good (RSD = 3.7%, $n = 5$). To study the reproducibility of the fabricated sensor, different AuNP/SPCE sensors were fabricated and tested under identical conditions. The value of RSD associated with measurements with these sensors was found to be less than 10%, which is good considering that no effort has been made to optimize/standardize the sensor fabrication.

The performances of the modified AuNP/SPCE electrode on different days in the presence of dopamine have been also monitored. Results in Figure 10 indicated that the response of the sensor on the second day is almost similar to, or even better than, that on the first day, which suggests the good stability of the electrode sensor. Under these experimental conditions, the relative standard deviation to 50 μM DA was
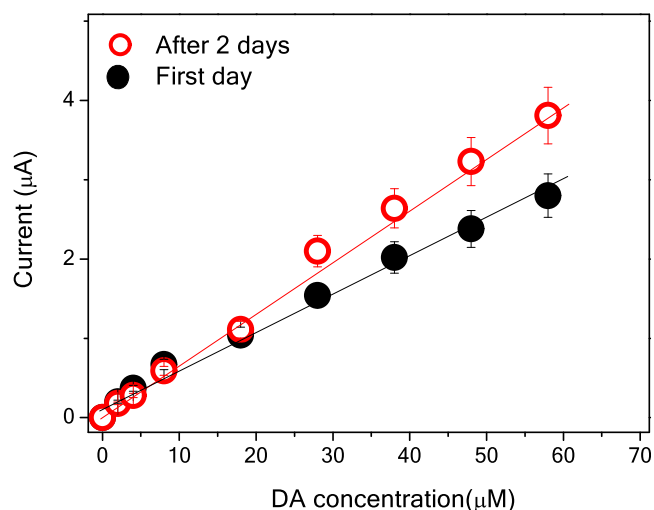

Figure 10. Calibration curves for DA with AuNP/SPCE tested on different days.

approximately 9.36%, which indicated that the method has also good reproducibility.

To compare the sensing performances for dopamine and riboflavin detection with the modified electrode vs previous electrochemical sensors reported in the literature, in Table 1 are summarized the relevant characteristics of these sensors, i.e., the linear range and limit of detection.

By this comparison, we can deduce that our sensor demonstrates almost comparable performances with respect to the state-of-the-art sensors for DA and RF sensing.

2.4. Real Sample Analysis. To evaluate the capability of the proposed modified SPCE sensor for dopamine measurement in a real sample, we tested a dopamine-based pharmaceutical formulation (S.A.L.F. Company, Bergamo, Italy). The LSV voltammetric method has been utilized for its simplicity. Before measurements, the sample was properly diluted with 0.1 M PBS solution to reach a concentration value that fits into the linear range. The determination of DA was performed using the standard addition method. The recovery percent was in the range 96−104% ($n = 3$, see Table 2), which indicates the accuracy and repeatability of the proposed method also in a real complex matrix.

3. EXPERIMENTAL SECTION

3.1. Preparation of *R. suaveolens* Extract. The extract of *R. suaveolens* was obtained as follows. First, *R. suaveolens* aerial parts were harvested in March 2018, cleaned with tap water, and dried under shade for one week. The dried plant was ground into coarse powder by a mechanical grinder. The coarse powder was then subject to maceration with methanol (100%) for 72 h and filtered. The filtrates were pooled, and the solvent was removed using a rotary evaporator. The concentrated extract was stored at 4 °C. More information about this procedure can be found in ref 18.

3.2. Synthesis of AuNPs. AuNPs were obtained through the simple procedure shown in Scheme 1 by adding, drop by drop, 5 mL of methanolic *R. suaveolens* extract (6.67 mg mL^{-1}) to 45 mL of 1 mM aqueous solution of HAuCl$_4$ at room temperature under stirring conditions. Before the extract was added, the color of the HAuCl$_4$ solution was pale yellow. Within 15 min, the solution color changed to purple-red, indicating the successful reduction of Au ions to AuNPs.

Table 1. Comparison of AuNP/SPCE Sensor Performance with Recently Reported Dopamine and Riboflavin Electrochemical Sensors

sensor	analyte	linear range	LOD	refs
Au/RGO/GCE	DA	6.8−41 μM	1.4 μM	42
PANI-GO/GCE	DA	2−18 μM	0.5 μM	43
graphene nanosheets (GNSs)	DA	4−52 μM	0.6 μM	44
NdFeO$_3$	DA	0.5−100 μM	270 nM	45
LaFeO$_3$	DA	0.02−1.6 μM	59 nM	46
AuNP/SPCE	DA	2−100 μM	0.22 μM	this work
Cr-SnO$_2$	RF	0.2 nM−0.1 mM	0.11 nM	31
ssDNA-MoS$_2$-GN	RF	25 nM−2.25 mM	20 nM	47
carbon cloth (CC)	RF	5−100 nM	2.2 nM	48
MnO$_2$	RF	20 nM−9 μM	15 nM	49
Co^{2+}-Y zeolite	RF	1.7−3.4 μM	0.71 μM	50
MoS$_2$-MoO$_3$CC	RF	2−40 μM	15 nM	51
AuNP/SPCE	RF	2−70 μM	0.067 μM	this work

Table 2. Results from the Determination of DA with the AuNP/SPCE Sensor in a Real Integrator Sample[a]

sensor	expected (mg DA/tablet) (mg)	found (mg DA/tablet) (mg)	recovery[b] (%)
	500	522	104.4
AuNP/SPCE	500	479	95.8
	500	493	98.6

[a]The RSD (%) calculated for these measurements was 3.9 (n = 3). [b]Recovery values were evaluated as follows: Recovery (%) = (mg DA found/mg DA expected) × 100.

3.3. Characterization.
UV−vis measurements were performed by a Jasco V-570 PerkinElmer Lambda 1050 instrument. Scanning electron microscopy (SEM) analysis was performed by a 1540XB Zeiss field-emission SEM (FESEM) instrument operating at 10 kV. Transmission electron microscopy (TEM) analysis was carried out with a Philips CM12 instrument equipped with an Oxford EDX system for quantitative elemental analysis. The particle size distribution was measured using a dynamic light scattering (DLS) instrument (Zetasizer Nano ZS ZEN3600, Malvern, U.K.).

3.4. Modified Electrode Fabrication.
Screen-printed carbon electrodes (SPCEs) were purchased from DropSens, Spain. The SPE platform used was DRP-100 (named SPCE), constituted of a 4 mm diameter carbon working electrode, a silver pseudo-reference electrode, and a carbon auxiliary electrode. To modify the bare SPCE, a certain volume of AuNPs at a concentration of 5 mg/mL was directly drop cast onto the surface of the working electrode and left at room temperature to dry until further use.

3.5. Electrochemical Test.
Electrochemical analyses (cyclic voltammetry (CV) and linear sweep voltammetry (LSV)) were performed by a DropSens μStat 400 potentiostat empowered by Dropview 8400 software for data acquisition. CV tests were carried out in aerated 1 M PBS as the electrolyte at a scan rate of 50 mV s^{-1} in the potential range from −1 to −1 V by varying the concentration of the investigated analytes (0−500 μM). Calibration curves were obtained by plotting the faradic current vs analyte concentration. The sensitivity was computed as the slope of the calibration curve, and the limit of detection (LOD) was computed at S/N = 3. Both the sensitivity and limit of detection were evaluated within the linear range of the calibration curve. All experiments were performed at room temperature.

■ AUTHOR INFORMATION

Corresponding Author
Giovanni Neri − *Department of Engineering, University of Messina, I-98166 Messina, Italy;* ⊙ orcid.org/0000-0001-8999-060X; Email: gneri@unime.it

Authors
Sabrine Chelly − *Laboratory of Toxicology-Microbiology Environmental and Health, LR17ES06, Sfax Faculty of Sciences, University of Sfax, 3000 Sfax, Tunisia*

Meryam Chelly − *Laboratory of Toxicology-Microbiology Environmental and Health, LR17ES06, Sfax Faculty of Sciences, University of Sfax, 3000 Sfax, Tunisia*

Rayhane Zribi − *Department of Engineering, University of Messina, I-98166 Messina, Italy*

Radhouane Gdoura − *Laboratory of Toxicology-Microbiology Environmental and Health, LR17ES06, Sfax Faculty of Sciences, University of Sfax, 3000 Sfax, Tunisia*

Hanen Bouaziz-Ketata − *Laboratory of Toxicology-Microbiology Environmental and Health, LR17ES06, Sfax Faculty of Sciences, University of Sfax, 3000 Sfax, Tunisia*

Complete contact information is available at:
https://pubs.acs.org/10.1021/acsomega.1c00793

Author Contributions
S.C. and M.C. contributed equally to this work. The manuscript was written through the contribution of all authors. All authors have given approval to the final version of the manuscript.

Notes
The authors declare no competing financial interest.

■ REFERENCES

(1) Rajasekhar, C.; Kanchi, S. Green Nanomaterials for Clean Environment. In *Handbook of Ecomaterials*; Martínez, L.; Kharissova, O.; Kharisov, B., Eds.; Springer, 2018.

(2) Chaudhary, K.; Mogha, N. K.; Lalwani, S.; Sharma, R. K.; Masram, D. T. Ruthenium oxide nanoparticles immobilized over *Citrus limetta* waste derived carbon material for electrochemical detection of hexestrol. *J. Mater. Chem. B* **2020**, *8*, 7956−7965.

(3) Chaithra, K. P.; Vinay, S. B.; Akshaya, K. B.; Maiyalagan, T.; Hegde, G.; Varghese, A.; George, L. Unique Host Matrix to Disperse Pd Nanoparticles for Electrochemical Sensing of Morin: Sustainable Engineering Approach. *ACS Biomater. Sci. Eng.* **2020**, *6*, 5264−5273.

(4) Duan, H.; Wang, D.; Li, Y. Green chemistry for nanoparticle synthesis. *Chem. Soc. Rev.* **2015**, *44*, 5778−5792.

(5) Makarov, V.; Love, A.; Sinitsyna, O.; Makarova, S.; Yaminsky, I.; Taliansky, M.; Kalinina, N. "Green" nanotechnologies: synthesis of metal nanoparticles using plants. *Acta Naturae* **2014**, *6*, 21−28.

(6) Iravani, S. Green synthesis of metal nanoparticles using plants. *Green Chem.* **2011**, *13*, 2638.

(7) Guo, S.; Wang, E. Synthesis and electrochemical applications of gold nanoparticles. *Anal. Chim. Acta* **2007**, *598*, 181−192.

(8) Shah, M.; Badwaik, V.; Kherde, Y.; Waghwani, H. K.; Modi, T.; Aguilar, Z. P.; Rodgers, H.; Hamilton, W.; Marutharaj, T.; Webb, C.; Lawrenz, M. B.; Dakshinamurthy, R. Gold nanoparticles: various methods of synthesis and antibacterial applications. *Front. Biosci.* **2014**, *19*, 1320−1344.

(9) Goia, D. V.; Matijevic, E. Preparation of monodispersed metal particles. *New J. Chem.* **1998**, *22*, 1203−1215.

(10) Teimuri-mofrad, R.; Hadi, R.; Tahmasebi, B.; Farhoudian, S.; Mehravar, M.; Nasiri, R. Green synthesis of gold nanoparticles using plant extract: Mini-review. *Nanochem. Res.* **2017**, *2*, 8−19.

(11) Chandran, S. P.; Chaudhary, M.; Pasricha, R.; Ahmad, A.; Sastry, M. Synthesis of gold nanotriangles and silver nanoparticles using *Aloe vera* plant extract. *Biotechnol. Prog.* **2006**, *22*, 577−583.

(12) Das, R. K.; Borthakur, B. B.; Bora, U. Green synthesis of gold nanoparticles using ethanolic leaf extract of *Centella asiatica*. *Mater. Lett.* **2010**, *64*, 1445−1447.

(13) Song, J. Y.; Jang, H.-K.; Kim, B. S. Biological synthesis of gold nanoparticles using *Magnolia kobus* and *Diopyros kaki* leaf extracts. *Process Biochem.* **2009**, *44*, 1133−1138.

(14) Ghodake, G. S.; Deshpande, N. G.; Lee, Y. P.; Jin, E. S. Pear fruit extract-assisted room-temperature biosynthesis of gold nano-plates. *Colloids Surf., B* **2010**, *75*, 584−589.

(15) He, S.; Zhang, Y.; Guo, Z.; Gu, N. Biological Synthesis of Gold Nanowires Using Extract of *Rhodopseudomonas* capsulata. *Biotechnol. Prog.* **2008**, *24*, 476−480.

(16) Krpetić, Ž.; Scar, G.; Caneva, E.; Speranza, G.; Porta, F. Gold Nanoparticles Prepared Using *Cape Aloe* Active Components. *Langmuir* **2009**, *25*, 7217−7221.

(17) Alegria, E.; Ribeiro, A.; Mendes, M.; Ferraria, A.; Rego, A. M.; Pombeiro, A. Effect of Phenolic Compounds on the Synthesis of Gold Nanoparticles and its Catalytic Activity in the Reduction of Nitro Compounds. *Nanomaterials* **2018**, *8*, 320.

(18) Chelly, S.; Chelly, M.; Salah, H. B.; Athmouni, K.; Bitto, A.; Sellami, H.; Kallel, C.; Bouaziz-Ketata, H. HPLC-DAD Analysis, Antioxidant and Protective Effects of Tunisian *Rhanterium suaveolens* against Acetamiprid Induced Oxidative Stress on Mice Erythrocytes. *Chem. Biodiversity* **2019**, *16*, No. e1900428.

(19) Mittal, A. K.; Chisti, Y.; Banerjee, U. C. Synthesis of metallic nanoparticles using plant extracts. *Biotechnol. Adv.* **2013**, *31*, 346−56.

(20) Kim, E. Y.; Kumar, D.; Khang, G.; Lim, D.-K. Recent advances in gold nanoparticle-based bioengineering applications. *J. Mater. Chem. B* **2015**, *3*, 8433−8444.

(21) Cooper, J. R.; Bloom, F. E.; Roth, R. H. *The Biochemical Basis of Neuropharmacology*; Oxford University Press: New York, 1986.

(22) Powers, H. J. Riboflavin (vitamin B-2) and health. *Am. J. Clin. Nutr.* **2003**, *77*, 1352.

(23) Chandra, S.; Siraj, S.; Wong, D. K. Y. Recent Advances in Biosensing for Neurotransmitters and Disease Biomarkers using Microelectrodes. *ChemElectroChem* **2017**, *4*, 822−833.

(24) Bala, K.; Sharma, D.; Gupta, N. Carbon-Nanotube-Based Materials for Electrochemical Sensing of the Neurotransmitter Dopamine. *ChemElectroChem* **2019**, *6*, 274−288.

(25) Maduraiveeran, G.; Sasidharan, M.; Ganesan, V. Electrochemical sensor and biosensor platforms based on advanced nanomaterials for biological and biomedical applications. *Biosens. Bioelectron.* **2018**, *103*, 113−129.

(26) Lavanya, N.; Leonardi, S. G.; Sekar, C.; Ficarra, S.; Galtieri, A.; Tellone, E.; Neri, G. Detection of Catecholamine Neurotransmitters by Nanostructured SnO2-Based Electrochemical Sensors: A Review of Recent Progress. *Mini-Rev. Org. Chem.* **2018**, *15*, 382−388.

(27) Tertiş, M.; Florea, A.; Adumitrachioaie, A.; Cernat, A.; Bogdan, D.; Barbu-Tudoran, L.; Jaffrezic Renault, N.; Sandulescu, R.; Cristea,

C. Detection of Dopamine by a Biomimetic Electrochemical Sensor Based on Polythioaniline-Bridged Gold Nanoparticles. *ChemPlusChem* **2017**, *82*, 561−569.

(28) Sumathi, C.; Muthukumaran, P.; Radhakrishnan, S.; Ravi, G.; Wilson, J. Riboflavin detection by *α*-Fe2O3/MWCNT/AuNPs-based composite and a study of the interaction of riboflavin with DNA. *RSC Adv.* **2015**, *5*, 17888.

(29) Negut Cioates, C. Review - Electrochemical Sensors Used in the Determination of Riboflavin. *J. Electrochem. Soc.* **2020**, *167*, No. 037558.

(30) Derakhshan, M.; Shamspur, T.; Molaakbari, E.; Mostafavi, A.; Saljooqi, A. Fabrication of a Novel Electrochemical Sensor for Determination of Riboflavin in Different Drink Real Samples. *Russ. J. Electrochem.* **2020**, *56*, 181−188.

(31) Lavanya, N.; Radhakrishnan, S.; Sekar, C.; Navaneethan, M.; Hayakawa, Y. Fabrication of Cr doped SnO2 nanoparticles based biosensor for the selective determination of riboflavin in pharma-ceuticals. *Analyst* **2013**, *138*, 2061.

(32) Wahab, M. A.; Darain, F.; Karim, M. A.; Beltramini, J. N. Nano-confined Synthesis of Highly Ordered Mesoporous Carbon and its Performance as Electrode Material for Electrochemical Behavior of Riboflavin (Vitamin B2) and Dopamine. *Int. J. Electrochem. Sci.* **2015**, *10*, 7732−7742.

(33) Tigari, G.; Manjunatha, J. G. A surfactant enhanced novel pencil graphite and carbon nanotube composite paste material as an effective electrochemical sensor for determination of riboflavin. *J. Sci.: Adv. Mater. Devices* **2020**, *5*, 56−64.

(34) Taleat, Z.; Khoshroo, A.; Mazloum-Ardakani, M. Screen-printed electrodes for biosensing: a review (2008−2013). *Microchim. Acta* **2014**, *181*, 865−891.

(35) Lavanya, N.; Sekar, C.; Ficarra, S.; Tellone, E.; Bonavita, A.; Leonardi, S. G.; Neri, G. A novel disposable electrochemical sensor for determination of carbamazepine based on Fe doped SnO2 nanoparticles modified screen-printed carbon electrode. *Mater. Sci. Eng. C* **2016**, *62*, 53−60.

(36) Haiss, W.; Thanh, N. T.; Aveyard, J.; Fernig, D. G. Determination of Size and Concentration of Gold Nanoparticles from UV−Vis Spectra. *Anal. Chem.* **2007**, *79*, 4215−4221.

(37) Mukha, I.; Vityuk, N.; Severynovska, O.; Eremenko, A.; Smirnova, N. The pH-Dependent Stucture and Properties of Au and Ag Nanoparticles Produced by Tryptophan Reduction. *Nanoscale Res. Lett.* **2016**, *11*, No. 101.

(38) Zheng, T.; Bott, S.; Huo, Q. Techniques for Accurate Sizing of Gold Nanoparticles Using Dynamic Light Scattering with Particular Application to Chemical and Biological Sensing Based on Aggregate Formation. *ACS Appl. Mater. Interfaces* **2016**, *8*, 21585−21594.

(39) Dhamecha, D.; Jalalpure, S.; Jadhav, K. *Nepenthes khasiana* mediated synthesis of stabilized gold nanoparticles: Characterization and biocompatibility studies. *J. Photochem. Photobiol., B* **2016**, *154*, 108−117.

(40) Mazloum-Ardakani, M.; Rajabi, H.; Beitollahi, H.; Mirjalili, B. F.; Akbari, A.; Taghavinia, N. Voltammetric Determination of Dopamine at the Surface of TiO2 Nanoparticles Modified Carbon Paste Electrode. *Int. J. Electrochem. Sci.* **2010**, *5*, 147.

(41) Chelly, M.; Chelly, S.; Zribi, R.; Bouaziz-Ketata, H.; Gdoura, R.; Lavanya, N.; Veerapandi, G.; Sekar, C.; Neri, G. Synthesis of Silver and Gold Nanoparticles from Rumex roseus Plant Extract and Their Application in Electrochemical Sensors. *Nanomaterials* **2021**, *11*, 739.

(42) Wang, C.; Du, J.; Wang, H.; Zou, C. E.; Jiang, F.; Yang, P.; Du, Y. A facile electrochemical sensor based on reduced graphene oxide and Au nanoplates modified glassy carbon electrode for simultaneous detection of ascorbic acid, dopamine and uric acid. *Sens. Actuators, B* **2014**, *204*, 302−309.

(43) Manivel, P.; Dhakshnamoorthy, M.; Balamurugan, A.; Ponpandian, N.; Mangalaraj, D.; Viswanathan, C. Conducting polyaniline-graphene oxide fibrous nanocomposites: preparation, characterization and simultaneous electrochemical detection of ascorbic acid, dopamine and uric acid. *RSC Adv.* **2013**, *3*, 14428−14437.

(44) Liu, S. Q.; Sun, W. H.; Hu, F. T. Graphene nano sheet-fabricated electrochemical sensor for the determina-tion of dopamine in the presence of ascorbic acid using cetyltrimethylammonium bromide as the discriminating agent. *Sens. Actuators, B* **2012**, *173*, 497−504.

(45) Anajafi, Z.; Naseri, M.; Neri, G. Gas sensing and electro-chemical properties of rare earth ferrite, LnFeO3 (Ln = Nd, Sm), nanoparticles. *Ceram. Int.* **2020**, *46*, 26682−26688.

(46) Thirumalairajan, S.; Girija, K.; Ganesh, V.; Mangalaraj, D.; Ponpandian, N. Detection of the neurotransmitter dopamine by a glassy carbon electrode modified with self-assembled perovskite $LaFeO_3$ microspheres made up of nanospheres. *RSC Adv.* **2014**, *4*, 25957.

(47) Wang, Y.; Zhuang, Q.; Ni, Y. Fabrication of riboflavin electrochemical sensor based on homoadenine single-stranded DNA/molybdenum disulfide−graphene nanocomposite modified gold electrode. *J. Electroanal. Chem.* **2015**, *736*, 47−54.

(48) Si, R.-W.; Yang, Y.; Yu, Y.-Y.; Han, S.; Zhang, C.-L.; Sun, D.-Z.; Zhai, D.-D.; Liu, X.; Yong, Y.-C. Wiring Bacterial Electron Flow for Sensitive Whole-Cell Amperometric Detection of Riboflavin. *Anal. Chem.* **2016**, *88*, 11222.

(49) Mehmeti, E.; Stanković, D. M.; Chaiyo, S.; Švorc, L.; Kalcher, K. Manganese dioxide-modified carbon paste electrode for voltam-metric determination of riboflavin. *Microchim. Acta* **2016**, *183*, 1619.

(50) Nezamzadeh Ejhieh, A.; Pouladsaz, P. Voltammetric Determi-nation of Riboflavin Based on Electrocatalytic Oxidation at Zeo-lite-Modified Carbon Paste Electrodes. *J. Ind. Eng. Chem.* **2014**, *20*, 2146−2152.

(51) Zribi, R.; Foti, A.; Donato, M. G.; Gucciardi, P. G.; Neri, G. Fabrication of a Novel Electrochemical Sensor Based on Carbon Cloth Matrix Functionalized with MoO_3 and 2D-MoS_2 Layers for Riboflavin Determination. *Sensors* **2021**, *21*, 1371.